

Up-Converted Emission in a Series of Phenylazomethine Dendrimers with a Porphyrin Core

Xingzhong Yan and Theodore Goodson, III*

Department of Chemistry, University of Michigan, Ann Arbor, Michigan 48201

Takane Imaoka and Kimihisa Yamamoto

CREST project (JST) and Department of Chemistry, Keio University, Yokohama, Japan 223-8522

Received: December 27, 2004; In Final Form: March 8, 2005

The nonlinear optical and time-resolved properties of a series of phenylazomethine–porphyrin dendrimers are reported. The linear optical properties were also investigated, and the efficiency of the energy transfer process was obtained. Measurements were also carried out with the basic building-block molecules. The process of frequency up-converted emission was observed in these porphyrin dendrimers. The mechanism for this effect is investigated and related to the process of “hot-band” absorption in the phenylazomethine–porphyrin system. Time-resolved measurements also suggested efficient intramolecular vibrational energy redistribution in these systems. These properties suggest that the porphyrin dendrimers may also have applications in light harvesting of low-frequency photons, as well as in sensors.

Introduction

Investigations of organic dendrimers have attracted great attention because of their possible use as active components in advanced materials.^{1–7} In particular, their optical properties have become the focus of novel optoelectronic and biotechnological devices.^{3,6,8,9} For example, dendrimers have been used to generate frequency up-converted emission and light modulation through a two-photon absorption (TPA) process.⁸ Strong enhancement of two-photon absorption due to intramolecular interactions have been reported in conjugated dendrimers.⁹ In addition to the impressive TPA properties of the organic dendrimers, there is also the possibility of observing frequency up-converted emission as a result of “hot-band” excitation. This may be accomplished by significant population of high vibrational states of the molecule.¹⁰

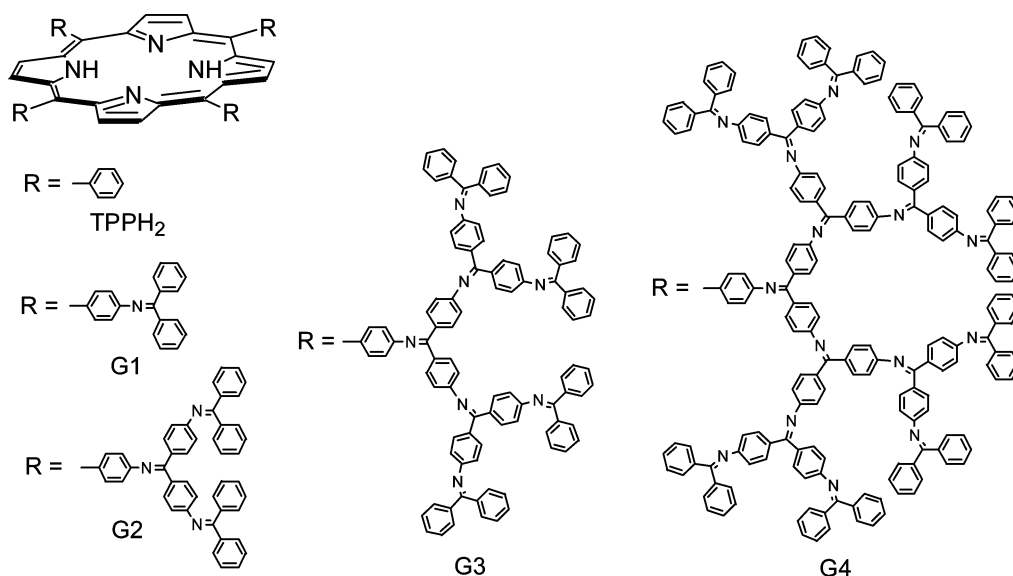
Hot-band excitation is a phonon cooperative single-photon process and can result in anti-Stokes fluorescence. This process has been reported in smaller organic systems.¹¹ For example, a study leading to the application of laser cooling was carried out by Rumbles et al.^{10,12} in xanthene laser dyes. Dendrimers offer a good architecture for chromophores which demonstrate hot-band absorption (HBA) because of the separation of the chromophore cores from each other by the dendrons. Dendrimers with porphyrin cores may also exhibit HBA because of the sublevel vibrational structure of the Q-bands.¹³ By introducing conjugated dendrons, efficient vibrational mode coupling in the system may be observed. This strategy may enhance HBA, resulting in a strong hot-band emission (HBE). HBA effects may bring about novel applications of these dendrimers for synthetic and biological systems because of its relatively large emission, which is comparable in magnitude to that of a two-photon induced emission (TPE) process.^{10–14} Other applications involving light harvesting of low-frequency photons,¹⁵ photodynamic therapy,¹⁴ and temperature sensors may also be possible.¹⁶

Fundamentally, understanding the nature of energy migration and charge separation in appropriate dendritic structures is essential.^{17–19} Conjugated porphyrin dendrimers have attracted great attention in this regard.^{20–23} For example, Yamamoto et al.²³ demonstrated a stepwise assembly of metal ions in a novel phenylazomethine-based metalloporphyrin dendrimer system. Novel applications of these dendrimers have been suggested for catalysis.²³ Modarelli et al.^{22a} synthesized a free-base porphyrin containing dendrimers with polyphenylene branches and benzoquinone end groups. This created a model system for photoinduced intramolecular charge transfer investigations.^{22a} Other conjugated porphyrin dendrimers with poly(platinum acetylide), polyphenyl, and stilbene dendrons have been developed particularly for the application of optoelectronics and artificial light harvesting.^{22b–e} Measurements of energy transfer (ET) efficiency and energy migration in these dendrimers have also been reported using steady-state spectroscopy.^{22b–e} Phenylazomethine dendrimers possess high thermal stability and rigidity due to the π -conjugated backbone and a high coordination ability of the imine nitrogen.^{1,23,24} These properties have led to novel metal ion assemblies²³ and electroluminescence devices.²⁴ The phenylazomethine dendrimer systems used in this study retain many of these important structural and electronic properties.

Shown in the Scheme 1 are the phenylazomethine–porphyrin dendrimers used in this study. We are interested in the energy transfer pathway. From the reports of steady-state measurements,^{22b–e} the ET pathway for particular porphyrin dendrimers may be understood by the following: The initial excitation is on the phenylazomethine dendrons in the UV. This is followed by energy transfer to the B-band of the porphyrin core. Excitation of the B-band in porphyrin may not necessarily lead to fluorescence to the ground state. Instead, it can lead to further energy transfer to the Q-band of the porphyrin. This may subsequently end in triplet-state emission of the excitation of the porphyrin core.^{20–22} The detailed investigation of this process using a set of complimentary experiments will give the necessary information to describe the energy flow in these dendrimers.

* To whom all correspondence should be addressed. E-mail: tgoodson@umich.edu.

SCHEME 1: Structures of Dendrimers



In this contribution, the optical properties of a series of phenylazomethine dendrimers with a free-base porphyrin core (Scheme 1) are reported. Frequency up-converted emission was observed at an excitation wavelength of 730 nm through thermally populated vibrational excited states. An HBA mechanism was suggested. The emission from an excitation at 820 nm was found to be due to a TPA process. Detailed measurements of the mechanism of energy transport in these porphyrin systems are carried out by fluorescence up-conversion and by steady-state spectroscopic measurements.

Experimental Section

General. UV-vis absorption spectra were recorded with a Hewlett-Packard 8452A diode array spectrophotometer. The fluorescence spectra were measured with a Shimadzu RF-1501 spectrofluorophotometer. The synthesis and analysis of structures and electronic properties of these dendrimers are given in ref 23. 5,10,15,20-Tetraphenyl-21*H*,23*H*-porphine (TPPH₂) was purchased from Aldrich. The dry solvents used for optical spectroscopic measurements were all deoxygenated by nitrogen.

Frequency Up-Converted Emission. The experiments were performed using a Ti:sapphire (Tsunami, Spectra Physics) femtosecond laser system pumped by a CW Nd:YVO₄ laser (Millennia, Spectra Physics). This system delivered stable light pulse sequences with individual pulse durations of ~ 57 fs and at a repetition rate of 82 MHz. The output spectrum of the laser radiation was monitored by a spectrum analyzer (Ocean Optics), which was used as a probe to ensure the pure mode-locking regime of the femtosecond laser. The laser beam was focused into the 1-cm quartz cell to induce fluorescence. The spot diameter size of the incident beam before the focus is ~ 3 mm, and the diameter of the airy disk at the focal point is ~ 17 μ m. The fluorescence was collected by an objective at focal point of the incident beam and at the direction perpendicular to that of the transmittance.^{25–27} The power dependence of the fluorescence intensity $F(P)$ may be modeled as^{14,25–27}

$$F(P) = K(\sigma_1\phi_1CL)P + \frac{1}{2}K\left(\frac{g}{f\tau}\frac{\pi}{2\lambda}\sigma_2\phi_2C\right)P^2 \quad (1)$$

in which K is an instrumental factor for fluorescence collection efficiency, subscripts 1 and 2 donate a single-photon and two-photon process, respectively, σ_1 is the one-photon absorption

cross-section (such as HBA; cm²/molecule), and σ_2 is the TPA cross-section (cm⁴·s/photon·molecule). ϕ_1 is single-photon emission (SPE) quantum yield, and ϕ_2 is the two-photon emission (TPE) quantum yield, C is the concentration of the solution (number of solute in cm³), the g factor is a dimensionless quantity only depending on the shape of the incident pulse (for a Gaussian temporal profile, $g = 0.664^{25}$), f is the pulse repetition rate (pulse/s; it is ~ 82 MHz), τ is the pulse width (s) (τ is estimated at ~ 100 fs for our setup), P is the average power of incident beam (photons/s), L is the effective path length (in cm) of the incident beam, and λ is the wavelength of the incident beam (in cm). Equation 1 can also be expressed as

$$F(P) = AP + BP^2 \quad (2)$$

Here, $A = K(\sigma_1\phi_1CL)$ and $B = \frac{1}{2}K\left(\frac{g}{f\tau}\frac{\pi}{2\lambda}\sigma_2\phi_2C\right)$. Thus, a correlation between HBA and TPA may be described by

$$\frac{A}{B} = 1.92(\lambda f \tau L) \frac{\sigma_1\phi_1}{\sigma_2\phi_2} \quad (3)$$

The frequency up-converted emission of these phenylazomethine dendrimers were measured at $\sim 10^{-4}$ – 10^{-5} M in tetrahydrofuran (THF). The TPE of rhodamine B with reported σ_2 and ϕ_2 values²⁵ was also measured as a standard.

Up-Conversion Fluorescence Decay. Time-resolved polarized fluorescence measurements for the dendrimer solutions were carried out using a femtosecond up-conversion technique. These solutions were prepared by dry, deoxygenated THF. The up-conversion system used in our experiments has been described in detail in previous reports.²⁸ Briefly, the sample solution was excited by the third harmonic (273 nm) light generating by mixing the second harmonic (410 nm) with the fundamental at a wavelength of 820 nm from the mode-locked Ti:sapphire laser pulses with a pulse width of ~ 57 fs (Tsunami, Spectra Physics). The polarization of the excitation beam for the anisotropy measurements was controlled with a Berek compensator. The rotating sample cell was used to avoid possible photodegradation and other accumulative effects. The fluorescence emitted from the sample was collected with an achromatic lens and directed onto a β -barium borate crystal. The fundamental light passes through a motorized optical delay line and then mixes with the sample emission in a nonlinear

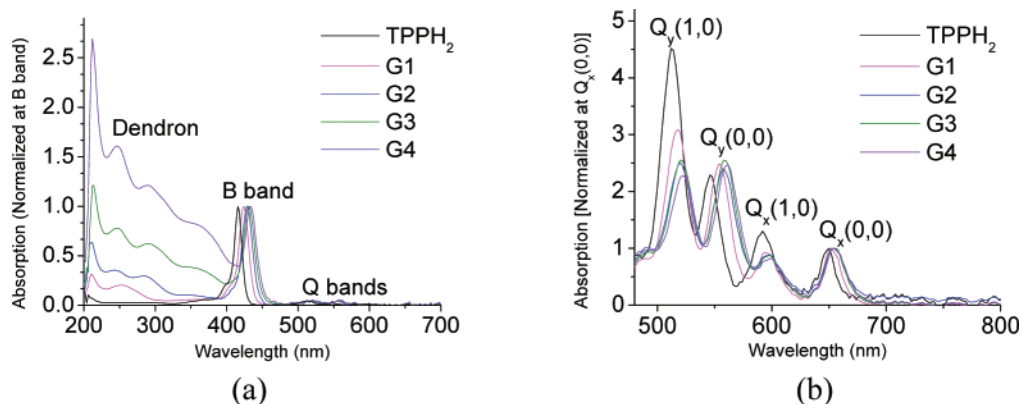


Figure 1. UV-vis absorption of G1–G4 and TPPH₂ in THF. (a) $\sim 10^{-5}$ M; (b) $\sim 10^{-3}$ M (showing Q-bands).

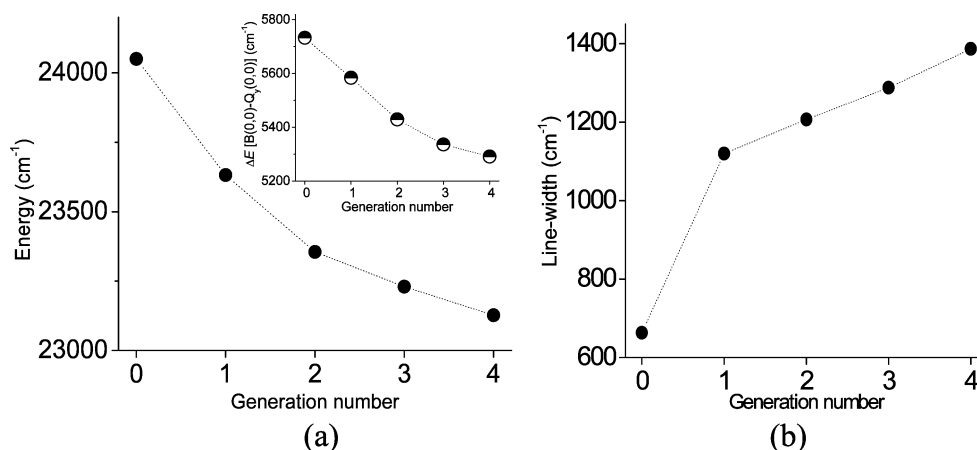


Figure 2. Transition energies for B-band and B–Q-band gap (a), and line widths (b) of the B-bands for the porphyrin core (The line widths (fwhms) were obtained by Gaussian fitting of the related absorption peaks, and TPPH₂ was treated as G0).

crystal to generate sum frequency light. The sum frequency light is dispersed using a monochromator and detected by a photomultiplier tube (Hamamatsu R1527P). The instrument response function (IRF) was estimated to be ~ 398 fs by the observation of the rise time for the fluorescence dynamics of different dyes in different solvents at an excitation wavelength of 273 nm.

Results and Discussion

A. UV-vis Absorption. Shown in Figure 1 are the absorption spectra of the porphyrin dendrimers dissolved in THF. The absorption peak at ~ 430 nm is attributed to the B-band (S_2) of the porphyrin core. The absorption band near ~ 520 nm is assigned to the Q-bands (S_1 of the porphyrin core). The higher-energy bands (at wavelengths less than 400 nm) are attributed to the absorption of the phenylazomethine dendrons. Also shown is the absorption spectrum of the TPPH₂ molecule in THF, which also has an absorption band at 416 nm (B-band) and others at wavelengths slightly blue-shifted from the Q-bands of the dendrimer.

The absorption bands below 300 nm are attributed to the π – π^* transitions of the phenylazomethine dendrons. These transitions are also close to the N-band of the porphyrin core.²⁹ In the vicinity of ~ 360 nm, there are n – π^* transitions from the dendrons as well.

For the case of the B-band absorption of the porphyrin core, a noticeable red-shift and a significant broadening of the line width were observed as a function of the dendrimer generation (Figure 2). A significant red-shift of ~ 18 nm (920 cm⁻¹) for the B-band of the porphyrin core was observed between TPPH₂ and the fourth-generation (G4) dendrimer. The Q-bands also

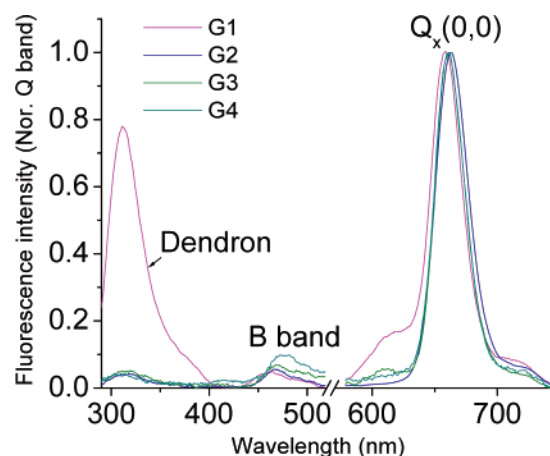


Figure 3. Emission spectra of G1–G4 with an excitation of 273 nm in THF.

showed a small red-shift with increasing generation number. The B(0,0)–Q_x(0,0) (S_2 – S_1) band gap was found to decrease by 440 cm⁻¹ from TPPH₂ to G4. Also shown in Figure 2 is the dependence of the line width of the B-band with increasing dendrimer generation. The line-width of the B-band for G1–G4 is $\sim 2\times$ that for TPPH₂. The shift in the B-band absorption as well as the increases in the line width as a function of the dendrimer generation may be related to the increasing interaction of the conjugated dendrons with the porphyrin core (see below).

B. Steady-State Emission and Energy Transfer. Shown in Figure 3 are the emission spectra (excitation wavelength 273 nm) for the porphyrin dendrimers of generation one to four (G1 to G4) dissolved in THF. For the G1 dendrimer, a relatively

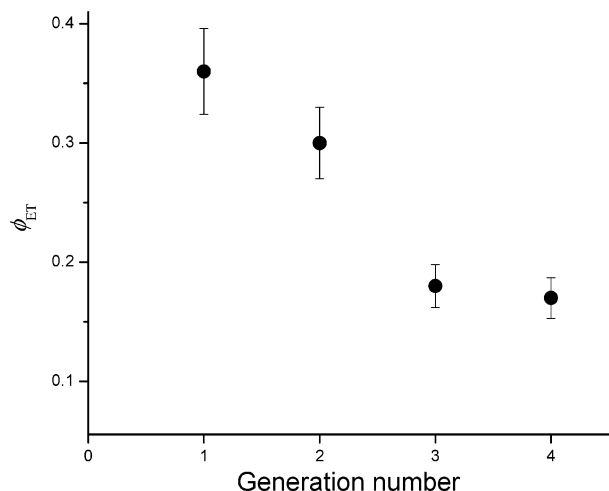


Figure 4. Generation dependence of the ET efficiency in the CHCl_3 solution with an excitation of 273 nm.

strong emission band at ~ 310 nm was observed and attributed to the emission of the phenylazomethine dendrons. For higher-generation dendrimers, the emission from the dendron was relatively weak. The Q-band emission ($Q_x(0,0)$ or S_1-S_0 transition) was observed at ~ 660 nm. The weak emission near ~ 470 nm may be attributed to the emission of the B-band or residual emission from the dendron (see below).

Because of the low quantum yield at the B-band, the emission from this band was difficult to detect.^{30,31} However, there was a small (residual) emission at ~ 470 nm as described above. Measurements at different excitation wavelengths (for example, at ~ 430 nm) suggested that the emission from direct excitation of the B-band was relatively small in comparison to the emission at the B-band through energy transfer from the dendrons (excitation 273 nm). Thus, this suggests that there is a small contribution of the energy transferred from the dendrons to the B-band, but the energy is not completely transferred to the Q-band.

The quantum yield of the Q-band emission for the different generations of porphyrin dendrimers (with excitation at the B-band) may be estimated by eq 4 in comparison to the emission of TPPH₂ in benzene ($\phi_{\text{TPPH}_2} \approx 0.11$)³²

$$\phi_d = \left(\frac{F_d}{F_{\text{TPPH}_2}} \right) \left(\frac{A_{\text{TPPH}_2}}{A_d} \right) \left(\frac{n_{\text{TPPH}_2}}{n_d} \right) \phi_{\text{TPPH}_2} \quad (4)$$

Here, ϕ , F , A , and n are the emission quantum yield, the integrated fluorescence and absorption, and the refractive index of solution, respectively. The subscript d denotes that the parameter is for the dendrimer. The quantum yield of the dilute THF dendrimer solutions (concentration $< 2 \times 10^{-6}$ M) was found to be 0.09 ± 0.01 , 0.15 ± 0.01 , 0.10 ± 0.02 , and 0.10 ± 0.01 for G1, G2, G3, and G4, respectively. We also found that when the excitation wavelength is near ~ 420 nm the quantum yield is higher than that for the case for direct excitation of the B-band. G2 shows the highest quantum yield, and other dendrimers possess almost the same quantum yield as TPPH₂ (0.10 ± 0.01) in THF.

The ET efficiency (ϕ_{ET} , the quantum yield for an excitation at 273 nm) may be estimated by the ratio of the normalized emission and absorption from the normalized excitation and absorption spectra at the B-band wavelength.^{22d} In comparison to the absorption and excitation spectra of G1, the ϕ_{ET} at the excitation wavelength of 273 nm is $\sim 36\%$, while that for G2, G3, and G4 is 30%, 18%, and 17%, respectively (Figure 4).

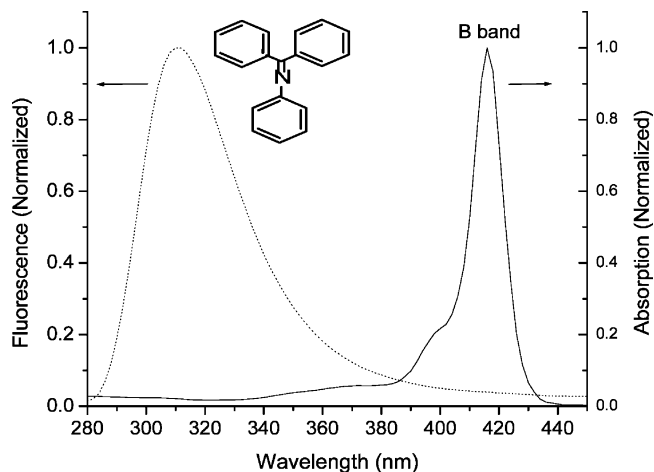


Figure 5. Spectral overlap of the emission of phenyl-ended phenylazomethine and absorption of B-band of TPPH₂.

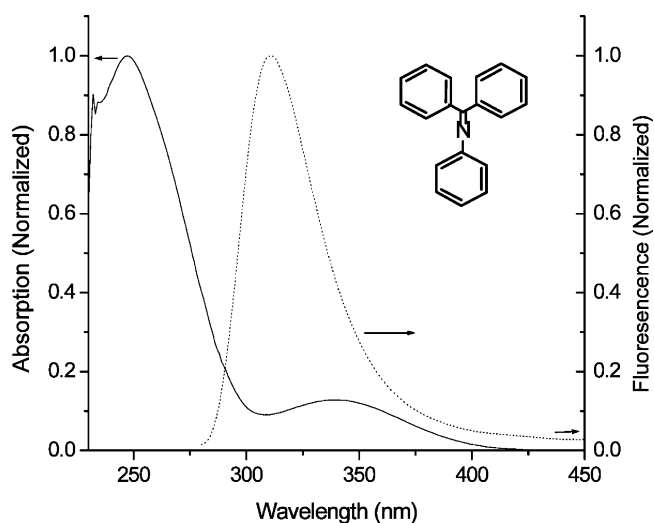


Figure 6. Spectral overlap of the absorption and emission of phenyl-ended phenylazomethine.

This suggests that, in general, the transfer efficiency is not as high as that in other light-harvesting macromolecules.¹⁷ This was surprising because the emission from dendrons was relatively weak for the higher generations.

However, one observes a relatively small overlap of the B-band absorption with the emission of the dendrons (Figure 5), which is suggestively the corporate for the small ET efficiency. Again, another important factor to be considered in the case of these dendrimers is that the broad absorption of the phenylazomethine dendrons may also result in self-absorption. Shown in Figure 6 is the absorption and emission spectra of the building-block molecule of the dendrons. As observed in the right panel of Figure 6, the absorption of the dendrons does overlap the emission quite well. This suggests that the ET efficiency to some extent may also be affected by reabsorption. For these dendrimers, the mechanisms for the dissipation of the energy may also include intramolecular vibrational energy redistribution (IVR)³³ and the generation of the triplet state³⁴ in the dendron system.

Assuming that a Förster mechanism³⁵ governs the energy transfer process, the electronic coupling between the donor and the acceptor can be described as a Coulombic interaction, which may be approximated as a dipole–dipole interaction between the transition dipole moments of the donor and the acceptor.³⁶ The ET rate $k_{ET}(r)$ is given by^{35–37}

$$k_{\text{ET}}(r) = \frac{1}{\tau_{\text{ET}}} = \frac{1}{\tau_{\text{D}}} \left(\frac{R_0}{r} \right)^6 = \frac{1}{\tau_{\text{D}}} \left(\frac{\phi_{\text{ET}}}{1 - \phi_{\text{ET}}} \right) \quad (5)$$

where τ_{ET} is the energy transfer time, τ_{D} is the lifetime of the donor in the absence of the acceptor, and r is the distance between the donor and the acceptor. The Förster radius R_0 (the effective interaction radius) is given by³⁷

$$R_0^6 = \frac{9000 \cdot \ln 10}{128 \cdot \pi^5 \cdot N_{\text{A}}} \frac{\kappa^2 \Phi_{\text{D}}}{n^4} J(\lambda) \quad (6)$$

where κ^2 is a factor describing the relative orientation of the transition dipoles of the donor and the acceptor, Φ_{D} is the quantum yield of the dendrons, N_{A} is Avogadro's number, n is the index of refraction of the solvent (it is 1.4 for THF), and $J(\lambda)$ is the spectral overlap integral defined by

$$J(\lambda) = \frac{\int F_{\text{D}}(\lambda) \epsilon_{\text{A}}(\lambda) \lambda^4 d\lambda}{\int F_{\text{D}}(\lambda) d\lambda} \quad (7)$$

in which $\epsilon_{\text{A}}(\lambda)$ represents the molar extinction coefficient of the acceptor and $F_{\text{D}}(\lambda)$ denotes the donor (dendron) fluorescence spectrum.

From eq 6, it can be seen that R_0 strongly depends on the orientation factor κ between the two interacting chromophores. κ^2 can be set to $2/3$ for the usually assumed random orientation of the dendrons for the high generations.^{35,36} For the smaller generations, the dendron orientation relative to the porphyrin plane cannot be taken as random. In this case, the κ value may be calculated by eq 8 for a three-dimensional molecular structure³⁵

$$\kappa = \sin \theta_{\text{D}} \sin \theta_{\text{A}} \cos \varphi_{\text{DA}} - 2 \cos \theta_{\text{D}} \cos \theta_{\text{A}} \quad (8)$$

where φ_{DA} is the azimuthal angle between the involved transition dipole moment directions of the energy donor (D) and acceptor (A), and θ_{D} and θ_{A} are the angles between the corresponding dipole directions of D and A with the internuclear D–A axis, respectively. For smaller generations, the dendron may lie in a plane which is possibly perpendicular to the porphyrin plane, and thus, a very small κ value is anticipated, except for the case in which the transition dipole moment of the dendrons lies in the direction along with the $>\text{C}=\text{N}-$ bond to the porphyrin core.

Figure 5 shows the overlap between the B-band of the free-base porphyrin core and the emission of the dendron (phenyl-ended phenylazomethine). If a random orientation of the dendrons is considered, a $J(\lambda)$ value of $1.696 \times 10^{-14} \text{ cm}^3 \cdot \text{M}^{-1}$ is obtained. Because the fluorescence emission behavior of the dendron is similar to that of benzophenone,³⁸ the Förster radius was estimated to be $\sim 8.0 \text{ \AA}$ for the case with a random orientation of the chromophores. The distance from the periphery (outside dendrons) to the core can be estimated by the bond lengths. For G1, it is about 12 \AA , and a stepwise increment of $\sim 8.1 \text{ \AA}$ for other higher generations may be used as an approximation. Thus, the ET rate was estimated to be less than 10^6 s^{-1} for all the generations (G1 to G4). This ET process is on the time scale of a microsecond. This agrees with our observation of low ET efficiency (see above). Because of the poor Coulombic coupling between the dendron and the porphyrin core, the energy cannot be completely transferred. Thus, the excitation may relax through other pathways, such as IVR³³ and singlet–singlet annihilation³⁴ in the dendron system.

However, the absorption of the dendrons is very close to the N-band of the porphyrin core, which was found in the vicinity of $\sim 273 \text{ nm}$ with weak amplitude in chloroform as the solvent.²⁹ There may be a spatial overlap of the orbitals of the dendrons and the porphyrin core. Also, the distance from the periphery to the porphyrin core is less than 1.9 nm in these dendrimers, as estimated from bond lengths and a crystal structure of the similar phenylazomethine system.³⁹ G1 has a short interaction distance ($\sim 1.2 \text{ nm}$). Thus, the excitation energy of the dendrons may be transported along the bond length to the porphyrin core in the case for G1. Such a short-range interaction may be treated as an inter-chromophore orbital overlap-dependent interaction.⁴⁰ In this case, the nonequilibrium relaxation of the bath on the time scale of resonant energy transfer and mixing of the donor and acceptor states can lead to coherent dynamics.³⁶ The addition of the dendrons resulted in a significant change of the spectral shape for the porphyrin core (section A). The smallest generation may have the best orbital overlap and give rise to a strong short-range interaction. This may be the explanation as to the reason G1 showed a higher ϕ_{ET} than the other generations.

C. Frequency Up-Converted Emission. Shown in Figure 7 are the spectra of the absorption and emission of the $\text{Q}_{\text{A}}(0,0)$ band in the porphyrin dendrimers at an excitation wavelength of 730 nm . One immediately observes that at this wavelength the exciting energy is much lower ($\sim 1600 \text{ cm}^{-1}$) than the absorption maximum of the Q-band. Also, the energy of the excitation wavelength 730 nm ($\sim 13\,700 \text{ cm}^{-1}$) is $\sim 1450 \text{ cm}^{-1}$ lower than the emission maximum located at $\sim 660 \text{ nm}$ ($\sim 15\,150 \text{ cm}^{-1}$). This emission maximum was similar to that obtained from excitation at 273 nm as described above. It is found that the energy difference between the emission maximum and the excitation wavelength is $\sim 7\text{--}8$ times that of the thermal energy (207 cm^{-1}) of room temperature (kT). The combination of these features suggests that the emission observed in this case results from a frequency up-converted process.^{8–14}

Figure 8 shows the power dependence of the up-converted fluorescence intensities for the different generations measured. The log–log plots were fitted well by a linear function, and in all cases, the slope significantly deviated from 2.00, which is expected for a two-photon induced emission process.^{8,9,13} From these results, it is clear that this effect is not a quadratic process.

There are three possible mechanisms for the observation of frequency up-converted fluorescence.¹² The first mechanism is TPE mentioned above, which has attracted great attention for potential applications.^{41–44} Because many porphyrin structures possess a very high TPA cross-section,^{13,45,46} they are very promising materials for medical imaging and photodynamic therapy. In such cases, the absorption and fluorescence should be relatively insensitive to temperature and the fluorescence intensity proportional to the square of the excitation intensity. In our observations, the absorption of the dendrimer solutions is negligently small at 730 nm and far from the $\text{Q}(0,0)$ band maximum (Figures 1 and 7). The double frequency (located at 365 nm) of this excitation (730 nm) is also near the resonance absorption of the porphyrin core (at $\sim 430 \text{ nm}$) as well as the $n\text{--}\pi^*$ transition (at $\sim 360 \text{ nm}$) of the dendrons. However, the power dependence of the fluorescence intensity did not show the expected quadratic relationship, which is an indicative signature of a two-photon process (Figure 8).

Another likely mechanism is related to a delayed fluorescence through a bimolecular process in which triplet–triplet annihilation plays a prominent role.⁴⁷ In these particular dendrimer systems, it is possible to excite from the lowest vibrational level of the ground state S_0 to the lowest triplet state T_1 which has a longer lifetime (see below).^{31,32} This lifetime may be long

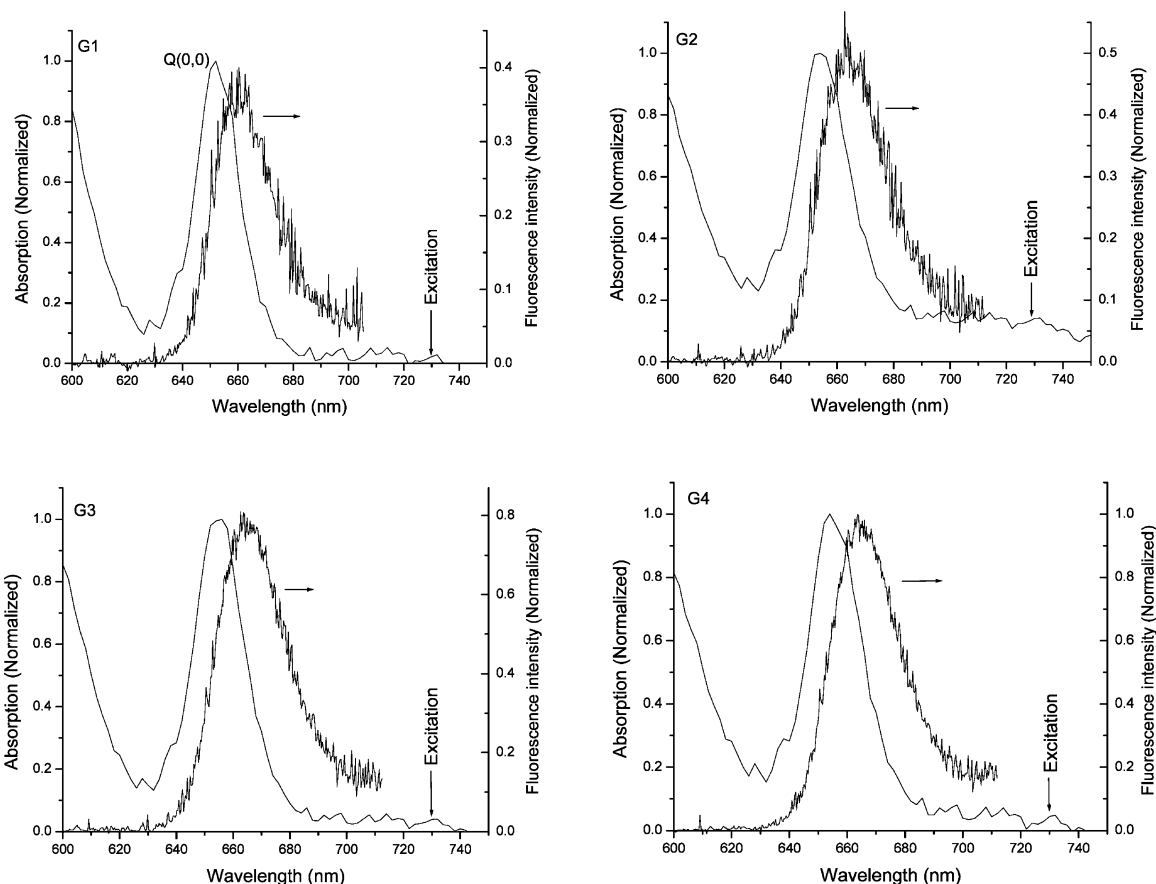


Figure 7. Up-converted emission of G1–G4 THF solutions ($\sim 6.0 \times 10^{-5}$ M) with an excitation at 730 nm and an induced power density of ~ 9.7 GW $\cdot\text{cm}^{-2}$ (Left: $Q_x(0,0)$ band absorption. Right: Up-converted emission spectra with a normalized intensity by the emission intensity of the G4 solution).

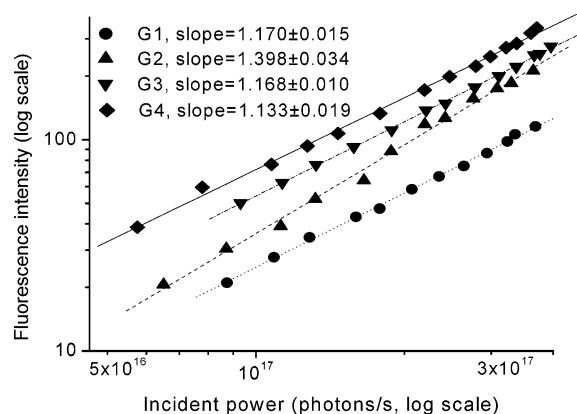


Figure 8. Power dependence of up-converted fluorescence with an excitation at wavelength of 730 nm.

enough to populate the first excited state S_1 by thermal activation of the triplet state T_1 . There are two features for this process: The lifetime of the luminescence should be equal to the lifetime of the triplet state, and the absorption coefficient should be independent of temperature.⁶ The temperature dependence of the absorption of these dendrimers (as measured in neat films of poly(vinyl butyral-co-vinyl alcohol-co-vinyl acetate) was not significant. However, no Stokes-shifted emission was detected, but instead, anti-Stokes emission (~ 660 nm) was observed, which is comparable to the steady-state $Q_x(0,0)$ transition (Figure 2). This anti-Stokes emission may originate from another process.

Finally, frequency up-converted emission may be observed as a result of HBE (i.e., populating of high vibrational states of

the molecule).^{10–12} Drobizhev et al.¹⁴ have recently observed this phenomenon in a *meso*-tetra-alkynylporphyrin system. Similar to their important report, the up-converted fluorescence from an excitation at 730 nm may suggest an HBA mechanism for the porphyrin dendrimers described here.

If the absorption of a photon excites a transition from one of the vibrational levels of the ground singlet state (S_0) to the lowest vibrational level of the first excited state (S_1) in the porphyrin core, the cross-section of the HBA may be estimated as the probability of a vibronic transition at the excited frequency, ν (eq 9)¹⁴

$$\sigma_1(\nu) = \sigma_1(\nu_{\max}) \exp\left(-\frac{\nu_{\max} - \nu}{kT}\right) \frac{FC(\nu)}{FC(\nu_{\max})} \quad (9)$$

where, $\sigma_1(\nu_{\max})$ is the cross-section at the band maximum which corresponds to the case of porphyrins excited in the $0 \leftarrow 0$ transition maximum, $FC(\nu)$ and $FC(\nu_{\max})$ are Franck–Condon factors for vibronic and $0 \leftarrow 0$ transitions, respectively. From the experimental parameters, ν is 13 700 cm^{-1} at the excitation wavelength of 730 nm, and kT is ~ 207 cm^{-1} at room temperature. The ratio $FC(\nu)/FC(\nu_{\max})$ may be estimated (after modeling) from the absorption coefficient located at $2\nu_{\max} - \nu$ and at ν_{\max} .¹⁴ After modeling the $Q_x(0,0)$ absorption with a Lorentzian function, this ratio was found to be 0.022, 0.034, 0.029, and 0.028 for G1, G2, G3, and G4, respectively. Therefore, the cross-section of HBA for these dendrimers can be calculated by the absorption spectral data. With rhodamine B at the same excitation ($\sigma_2 \approx 70$ GM and $\phi_2 \approx 0.7$ at 730 nm) as a standard,²⁵ the measurement was calibrated, and the cross-section for HBA was experimentally estimated to have a

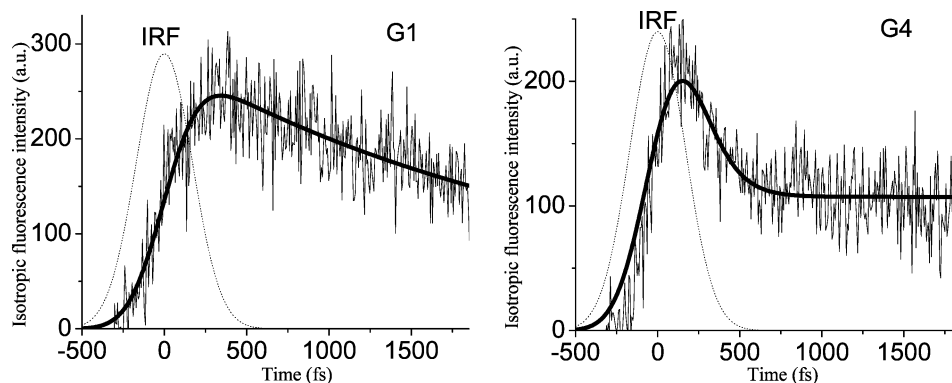


Figure 9. Fluorescence initial decay with the modeling curves for G1 and G4.

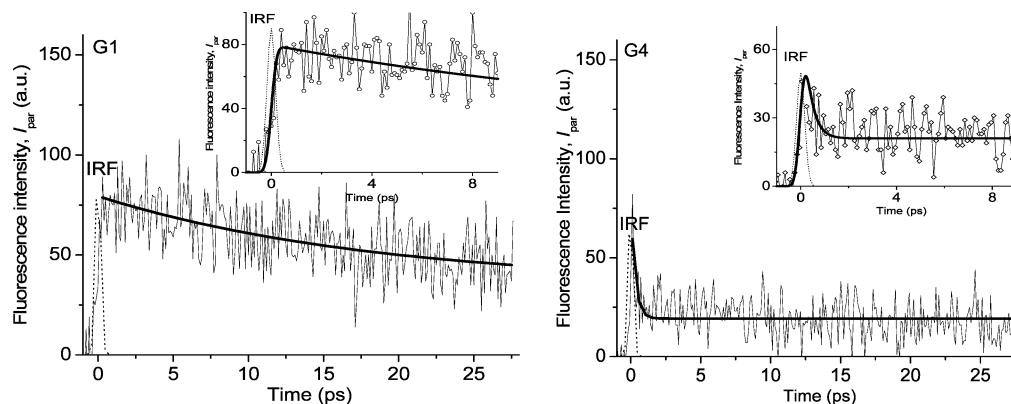


Figure 10. Long-time decay traces and corresponding fitting curves for G1 and G4 (Insert: Curves deconvoluted with the IRF for the first 10 ps).

TABLE 1: Cross-Sections of HBA and TPA at an Excitation of 730 nm^a

	ν_{\max} ($\times 10^4 \text{ cm}^{-1}$)	$\sigma_1(\nu_{\max})$ ($\times 10^{-17} \text{ cm}^2/\text{molecule}$)	$\sigma_1(\nu)$ ($\times 10^{-22} \text{ cm}^2/\text{molecule}$)	$\sigma_2(\nu)^b$ (GM)
G1	1.534	2.25	0.74	21.3
G2	1.531	3.00	1.08	
G3	1.529	2.79	1.65	40.2
G4	1.529	2.71	2.02	45.4

^a Concentration is 3.90×10^{16} , 3.73×10^{16} , 3.84×10^{16} , and 3.87×10^{16} molecules/cm³ for G1, G12, G3, and G4, respectively. ^b The cross-sections were obtained by modeling data for the emissions intensity. 1 GM = $10^{-50} \text{ cm}^4 \cdot \text{s} \cdot \text{molecule}^{-1} \cdot \text{photon}^{-1}$.

magnitude of $10^{-22} \text{ cm}^2 \cdot \text{molecule}^{-1}$ (Table 1). This agrees with the calculated results of the absorption spectra. These results suggest there is an HBA process for these dendrimers at an excitation wavelength of 730 nm.

In terms of the fitting in Figure 8, the slopes are not unity. This implies that the emission from the dendrimers does not originate from a purely linear process. The emission may also include other contributions such as a TPA process (nonlinear process).^{13,14} From the fitted data of the power-dependent fluorescence intensity plots (Figure 8), a cross-section of TPA was estimated using eq 3 (Table 1). These cross-sections of TPA are comparable to that of TPPH₂ (35 ± 20 GM) at an excitation of 730 nm.⁴⁵

It was also noted that the HBE intensity is dendrimer generation-dependent. G4 gave the strongest HBE intensity (Figures 7 and 8) and the highest HBA cross-section (Table 1). This may originate from an increase of the vibrational interaction in the system. There are two possible contributors for this process. One is a strong vibrational mode coupling both in vibrational levels of the dendrons³³ and in the porphyrin core.³¹ The other is a strong vibration interaction between the dendron

and the core,⁴⁸ which is possibly due to the increase of electronic interactions in the whole system. One can see that the energy gap ($\sim 1600 \text{ cm}^{-1}$) between the absorption band $Q_x(0,0)$ and the excitation (730 nm) is comparable to the energy for stretching vibrations of C=C and C=N bonds both in the dendron³⁹ and in the porphyrin core.⁴⁹ The energy gap (1453 cm^{-1}) between the excitation and the HBE band (660 nm) is also comparable to the magnitude for a totally symmetric vibration in the core ($\sim 1200\text{--}1600 \text{ cm}^{-1}$).⁴⁹ The thermal energy (207 cm^{-1}) is of the same order of magnitude as the lower-energy vibrational modes for porphyrins, such as the energy of a deformation vibrational mode in the porphyrin ring.⁵⁰ Because there may be a strong vibrational mode coupling in these dendrimers,^{33,48} an excitation of 730 nm can further populate the $Q_x(0,0)$ band by phonons through vibrational interactions. Such electron–phonon interaction was also observed in a dendrimer system with a photoisomerizable core.⁴⁸ The generation dependence for HBE in these dendrimers may be interpreted by the increase of the vibrational mode coupling with increasing dendrimer generation, which is connected with the electronic interactions between the dendrons and the porphyrin core.

Interestingly, the HBA process is not very efficient in the TPPH₂ small porphyrin molecule without dendrons. In comparison to the result of rhodamine B with a known σ_2 (~ 170 GM for the excitation at 820 nm and ~ 70 GM for the excitation at 730 nm) and a ϕ_2 of ~ 0.7 ,²⁵ the cross-section of the TPA for TPPH₂ was estimated to be 35 ± 20 GM and 5 ± 4 GM for an excitation at 730 and 820 nm, respectively. These results are in agreement with a previous report.⁴⁵ This gives further indication that the dendrons play an important role in the HBA properties. Also, the HBA process was also not observed in the dendrimer solutions with an excitation of 820 nm. Instead, a TPE process was observed in these dendrimers. In comparison to the TPE of a rhodamine B (1.2×10^{-4} M) methanol solution, the cross-

TABLE 2: Fast Components and Their Magnitudes for the Fluorescence Up-Conversion Results at the Excitation of 273 nm for the Dendrimer THF Solutions^a

	t_1/fs	A_1	t_1'/ps	A_1'
G1	2500	0.90	18.5	0.55
G2	2300	0.93	15.1	0.71
G3	180	0.85	1.00	0.57
G4	120	0.82	0.31	0.76

^a The time scale of the slow component (t_2 and t_2' for the initial and long time decay, respectively) is in the range ~ 10 – 12 ns.

section of TPA was found to be 33 ± 30 GM (8 GM/chromophore) for G1, 64 ± 23 GM (5.3 GM/chromophore) for G2, 238 ± 60 GM (8.5 GM/chromophore) for G3, and 334 ± 70 GM (5.6 GM/chromophore) for G4. These values are significantly larger than the TPA cross-section of TPPH₂ (5 ± 4 GM) and are also comparable to those of other porphyrins.^{13,45,46,51}

D. Fluorescence Dynamics with UV Excitation. With UV excitation (273 nm), the fluorescence decay results were recorded by fluorescence up-conversion spectroscopy^{28,37} for emission measured at 659 nm (at $Q_x(0,0)$) in THF solutions. Figures 9 and 10 show the initial and long-time fluorescence decay G1 and G4 dendrimers. The decay curves were deconvoluted with the IRF. The modeling results showed that the fluorescence decay of all the dendrimers possess two components, which included a fast component that was generation dependent. The slow component was also observed to have a time scale of ~ 10 ns (Table 2). This slow component can be attributed to the relaxation from the $Q_x(0,0)$ band to a triplet state.³² The fast component had two principle contributions. The first was observed with a time scale of 120–180 fs for G3 and G4 and approximately ~ 2 ps for G1 and G2. These decay times are similar to what was reported for IVR processes in rigid dendrimer systems.³³ They are also consistent with the time scale of the IVR process of the vibrational levels of the Q_x -bands for the porphyrin core.^{31,52} The fast components with a time scale under ~ 2.5 ps for the smaller-generation dendrimers may also include a solvent relaxation process, which may contain a vibrational energy redistribution induced by elastic collisions with solvent molecules.^{31,52} For the second time constant of the fast-decay process, there was also a generation dependence. The higher generations again were on the order of ~ 1 ps, while the first and second generations were much longer (15–18 ps). The longer times for G1 and G2 may be a result of thermal equilibration by energy exchange with the solvent.³¹

The observation of the generation dependence of the IVR process in the fluorescence dynamics may suggest that there is stronger vibrational mode coupling for the high-generation dendrimer than that for low generations. This enhancement for the vibrational mode coupling may be due to a strong electronic effect from the dendrons, such as the increase of the conjugation length and the overlap between the orbitals of the dendron and the N-band of the porphyrin core (section A). Also, an increase in the amplitude of HBE was observed, which correlates with the enhancement of the vibrational mode coupling for the high-generation dendrimers.

Conclusions

We have carried out steady-state, frequency up-converted emission and ultrafast spectroscopic measurements on a series of phenylazomethine dendrimers containing a free-base porphyrin core. Relatively low energy transfer efficiency may be the result of weak dipole–dipole interactions as suggested by

Förster theory. Hot-band absorption was observed for these dendrimers. The increase of the cross-section of hot-band absorption with an increase of the generation number is attributed to an enhanced intramolecular vibrational mode coupling in the dendrimer systems. Time-resolved studies also show an increase in intramolecular vibrational energy redistribution as a function of dendrimer generation resulting from vibrational mode coupling.

Acknowledgment. We thank the National Science Foundation (polymers), the Army Research Office (materials), and the Office of Naval Research for support of this investigation.

References and Notes

- (1) Nakajima, R.; Tsuruta, M.; Higuchi, M.; Yamamoto, K. *J. Am. Chem. Soc.* **2004**, *126*, 1630.
- (2) Li, Y.; Tseng, Y. D.; Kwon, S. Y.; d'Espaux, L.; Bunch, J. S.; McEuen, P. L.; Luo, D. *Nat. Mater.* **2004**, *3* (1), 38.
- (3) Sugiura, K. *Top. Curr. Chem.* **2003**, *228* (Dendrimers V), 65.
- (4) Bosman, A. W.; Jansen, H. M.; Meijer, E. W. *Chem. Rev.* **1999**, *99*, 1665.
- (5) Harth, E. M.; Hecht, S.; Helm, B.; Malmstrom, E. E.; Fréchet, J. M.; Hawker, C. J. *J. Am. Chem. Soc.* **2002**, *124*, 3926.
- (6) Ma, H.; Jen, Alex K.-Y. *Adv. Mater. (Weinheim, Ger.)* **2001**, *13* (15), 1201.
- (7) Ghaddar, T. H.; Wishart, J. F.; Thompson, D. W.; Whitesell, J. K.; Fox, M. A. *J. Am. Chem. Soc.* **2002**, *124*, 8285.
- (8) (a) Spangler, C. W.; Suo, Z.; Drobizhev, M.; Karotki, A.; Rebane, A. *NATO Sci. Ser. II: Math. Phys. Chem.* **2003**, *100* (Organic Nanophotonics), 139. (b) Adronov, A.; Fréchet, J. M. J.; He, G. S.; Kim, K.-S.; Chung, S.-J.; Swiatkiewicz, J.; Prasad, P. N. *Chem. Mater.* **2000**, *12*, 2838.
- (9) (a) Drobizhev, M.; Karotki, A.; Dzenis, Y.; Rebane, A.; Suo, Z.; Spangler, C. W. *J. Phys. Chem. B* **2003**, *107* (31), 7540. (b) Suo, Z.; Spangler, C. W.; Drobizhev, M.; Karotki, A.; Dzenis, Y.; Rebane, A. *Polym. Mater. Sci. Eng.* **2003**, *89*, 704. (c) Drobizhev, M.; Karotki, A.; Rebane, A.; Spangler, C. W. *Opt. Lett.* **2001**, *26* (14), 1081.
- (10) Clark, J. L.; Rumbles, G. *Phys. Rev. Lett.* **1996**, *76*, 2037.
- (11) Demchenko, A. P. *Luminescence* **2002**, *17*, 19.
- (12) Cark, J. L.; Miller, P. F.; Rumbles, G. *J. Phys. Chem. A* **1998**, *102*, 4428.
- (13) Kruk, M.; Karotki, A.; Drobizhev, M.; Kuzmitsky, V.; Gael, V.; Rebane, A. *J. Lumin.* **2003**, *105*, 45.
- (14) Drobizhev, M.; Karotki, A.; Kruk, M.; Krivokapic, A.; Anderson, H. L.; Rebane, A. *Chem. Phys. Lett.* **2003**, *370*, 690.
- (15) Metivier, R.; Kulzer, F.; Weil, T.; Mullen, K.; Basche, T. *J. Am. Chem. Soc.* **2004**, *126*, 14364.
- (16) Zander, C.; Drexchange, K. H. In *Advances in Photochemistry*; Neckers, D. C., Volman, D. H., von Bunau, G., Eds.; Wiley: New York, 1995; p 59.
- (17) For examples: (a) Adronov, A.; Fréchet, J. M. J. *J. Chem. Commun.* **2000**, 1701. (b) Serin, J. M.; Brousmiche, D. W.; J. M. J. *Chem. Commun.* **2002**, 2605. (c) Gilat, S. L.; Adronov, A.; Fréchet, J. M. J. *Angew. Chem., Int. Ed.* **1999**, *38* (10), 1422. (d) McClenaghan, N. D.; Passalacqua, R.; Loiseau, F.; Campagna, S.; Verheyde, B.; Hameurlaine, A.; Dehaen, W. *J. Am. Chem. Soc.* **2003**, *125*, 5356.
- (18) For examples: (a) Percec, V.; Glodde, M.; Bera, T. K.; Miura, Y.; Shiyankovskaya, I.; Singer, K. D.; Balagurusamy, V. S. K.; Heiney, P. A.; Schnell, I.; Rapp, A.; Spiess, H.-W.; Hudson, S. D.; Duan, H. *Nature (London)* **2002**, *419* (6905), 384. (b) Pogantsch, A.; Wenzl, F. P.; List, E. J. W.; Leising, G.; Grimsdale, A. C.; Mullen, K. *Adv. Mater.* **2002**, *14* (15), 1061. (c) Lor, M.; Thielemans, J.; Viaene, L.; Cotlet, M.; Hofkens, J.; Weil, T.; Hampel, C.; Mullen, K.; Verhoeven, J. W.; der Auwerda, M. V.; de Schryver, F. C. *J. Am. Chem. Soc.* **2002**, *124*, 9918.
- (19) For examples: (a) Yamamoto, K.; Higuchi, M.; Shiki, S.; Tsuruta, M.; Chiba, H. *Nature (London)* **2002**, *415* (6871), 509. (b) Bhyrappa, P.; Young, J. K.; Moore, J. S.; Suslick, K. S. *J. Am. Chem. Soc.* **1996**, *118*, 5708. (c) Bhyrappa, P.; Young, J. K.; Moore, J. S.; Suslick, K. S. *J. Mol. Catal. A* **1996**, *113*, 109. (d) Uyemura, M.; Aida, T. *J. Am. Chem. Soc.* **2002**, *124* (38), 11392.
- (20) Examples for dendritic porphyrins and porphyrin arrays: (a) Kim, M. J.; Tang, H.; Nikles, D. E. *Polym. Mater. Sci. Eng.* **2001**, *84*, 854. (b) del Rosario Benites, M.; Johnson, T. E.; Weghorn, S.; Yu, L.; Rao, P. D.; Diers, J. R.; Yang, S. I.; Kirmaier, C.; Bocian, D. F.; Holtz, D.; Lindsey, J. S. *J. Mater. Chem.* **2002**, *12* (1), 65. (c) Cho, H. S.; Rhee, H.; Song, J. K.; Min, C.-K.; Takase, M.; Aratani, N.; Cho, S.; Osuka, A.; Joo, T.; Kim, D. *J. Am. Chem. Soc.* **2003**, *125* (19), 5849. (d) Mak, C. C.; Pomeranc, D.; Sanders, J. K. M.; Montalti, M.; Prodi, L. *Chem. Commun.* **1999** (12), 1083. (e) Mongin, O.; Papamical, C.; Hoyler, N.; Gossauer, A. *J. Org. Chem.* **1998**, *63* (16), 5568.

- (21) Examples for nonconjugated dendrimers with porphyrin cores: (a) Hecht, S.; Vladimirov, Fréchet, J. M. J. *J. Am. Chem. Soc.* **2001**, *123*, 18. (b) Harth, E. M.; Hecht, S.; Helms, B.; Malmstrom, E. M.; Fréchet, J. M. J.; Hawker, C. J. *J. Am. Chem. Soc.* **2002**, *124*, 3926. (c) Pollak, K. W.; Leon, J. W.; Fréchet, J. M. J.; Maskus, M.; Abruna, H. D. *Chem. Mater.* **1998**, *10*, 30. (d) Rajesh, C. S.; Capitosti, G. J.; Cramer, S. J.; Modarelli, D. A. *J. Phys. Chem.* **2001**, *106*, 10175. (e) Choi, M.-S.; Aida, T.; Yamazaki, T.; Yamazaki, I. *Angew. Chem., Int. Ed.* **2001**, *40*, 3194; *Chem.—Eur. J.* **2002**, *8*, 2667.
- (22) Examples for conjugated dendrimers with porphyrin cores: (a) Capitosti, G. J.; Guerrero, C. D.; Binkley, D. E., Jr.; Rajesh, C. S.; Madarelli, D. A. *J. Org. Chem.* **2003**, *68*, 247. (b) Frampton, M. J.; Magennis, S. W.; Pillow, J. N. G.; Burn, P. L.; Sameuel, I. D. W. *J. Mater. Chem.* **2003**, *13*, 235. (c) Pillow, J. N. G.; Halim, M.; Lupton, J. M.; Burn, P. L.; Sameuel, I. D. W. *Macromolecules* **1999**, *32*, 5985. (d) Kimura, M.; Shiba, T.; Yamazaki, M.; Hanabusa, K.; Shirai, H.; Kobayashi, N. *J. Am. Chem. Soc.* **2001**, *123*, 5636. (e) Onitsuka, K.; Kitajima, H.; Fujimoto, M.; Iuchi, A.; Takei, F.; Takahashi, S. *Chem. Commun.* **2002**, 2576.
- (23) Imaoka, T.; Horiguchi, H.; Yamamoto, K. *J. Am. Chem. Soc.* **2003**, *125*, 340.
- (24) Sato, N.; Cho, J. S.; Higuchi, M.; Yamamoto, K. *J. Am. Chem. Soc.* **2003**, *125*, 8104.
- (25) Xu, C.; Webb, W. W. *J. Opt. Soc. Am. B* **1996**, *13*, 481.
- (26) Kennedy, S. M.; Lytle, F. E. *Anal. Chem.* **1986**, *58*, 2643.
- (27) Song, J. M.; Inoue, T.; Kawazumi, H.; Ogawa, T. *Anal. Sci.* **1999**, *15*, 601.
- (28) (a) Ranasinghe, M. I.; Wang, Y.; Goodson, T., III *J. Am. Chem. Soc.* **2003**, *125* (18), 5258. (b) Ranasinghe, M. I.; Varnavski, O. P.; Pawlas, J.; Hauck, S. I.; Louie, J.; Hartwig, J. F.; Goodson, T., III *J. Am. Chem. Soc.* **2002**, *124* (23), 6520. (c) Varnavski, O. P.; Ostrowski, J. C.; Sukhomlinova, L.; Twieg, R. J.; Bazan, G. C.; Goodson, T., III *J. Am. Chem. Soc.* **2002**, *124* (8), 1736.
- (29) Zhang, Q.; Wang, Z.; Liu, Y.; Zhu, Q.; Kong, F. *J. Chem. Phys.* **1996**, *105*, 5377.
- (30) (a) Seybold, P. G.; Gouterman, M. *J. Mol. Spectrosc.* **1969**, *31*, 1. (b) Quimby, D. J.; Longo, F. R. *J. Am. Chem. Soc.* **1975**, *97*, 5111.
- (31) Baskin, J. S.; Yu, H. Z.; Zewail, A. H. *J. Phys. Chem. A* **2002**, *106*, 9837.
- (32) Ohno, O.; Kaikoh, Y.; Kobayashi, H. *J. Chem. Phys.* **1985**, *82*, 1779.
- (33) Lor, M.; De, R.; Jordens, S.; De Belder, G.; Schweitzer, G.; Cotlet, M.; Hofkens, J.; Weil, T.; Herrmann, A.; Mllen, K.; Van Der Auweraer, M.; De Schryver, F. C. *J. Phys. Chem. A* **2002**, *106*, 2083.
- (34) Davadoss, C.; Bharathi, P.; Moore, J. *J. Am. Chem. Soc.* **1996**, *118*, 9635.
- (35) Förster, Th. *Ann. Phys.* **1948**, *2*, 55.
- (36) Scholes, G. D. *Annu. Rev. Phys. Chem.* **2003**, *54*, 57.
- (37) (a) Varnavski, O. P.; Goodson, T., III; *Chem. Phys. Lett.* **2000**, *320* 688. (b) Varnavski, O. P.; Leanov, A.; Liu, L.; Takacs, J.; Goodson, T., III *Phys. Rev. B* **2000**, *61*, 12732. (c) Varnavski, O. P.; Samuel, I. D. W.; Palsson, L. O.; Beavington, R.; Burn, P. L.; Goodson, T., III *J. Chem. Phys.* **2002**, *116*, 8893.
- (38) Turro, N. J. *Molecular Photochemistry*; W. A. Benjamin: New York, 1965. For benzophenone, the quantum yield is $<10^{-4}$ and lifetime is in a time scale of 10^{-6} s.
- (39) Higuchi, M.; Shiki, S.; Ariga, K.; Yamamoto K. *J. Am. Chem. Soc.* **2001**, *123*, 4414.
- (40) Scholes, G. D. *J. Phys. Chem.* **1996**, *100*, 18731.
- (41) Parthenopoulos, D. A.; Rentzepis, P. M. *Science* **1989**, *245*, 843.
- (42) Zhou, W.; Kuebler, S. M.; Braun, K. L.; Yu, T.; Cammack, J. K.; Ober, C. K.; Perry, J. W.; Marder, S. R. *Science* **2002**, *296*, 1106.
- (43) Kohler, R. H.; Cao, J.; Zipfel, W. R.; Webb, W. W. *Science* **1997**, *276*, 2039.
- (44) Bhawalkar, J. D.; Kumar, N. D.; Zhao, C. F.; Prasad, P. N. *J. Clin. Laser Med. Surg.* **1997**, *15*, 201.
- (45) Karotki, A.; Drobizhev, M.; Kruk, M.; Spangler, C.; Nickel, E.; Mamardashvili, N.; Rebane, A. *J. Opt. Soc. Am. B* **2003**, *20*, 321.
- (46) Ogawa, K.; Ohashi, A.; Kobuke, Y.; Kamada, K.; Ohta, K. *J. Am. Chem. Soc.* **2003**, *125*, 13356.
- (47) Samoc, A.; Samoc, M.; Davish, B. L. *Pol. J. Chem.* **2002**, *76*, 345.
- (48) Jiang, D. L.; Aida, T. *Nature (London)* **1997**, *388*, 454.
- (49) Hu, S.; Lin, C. H.; Blackwood, M. E., Jr.; Mukherjee, A.; Spiro, T. G. *J. Phys. Chem.* **1995**, *99*, 9694.
- (50) Klug, D. D.; Zgierski, M. Z.; Tse, J. S.; Liu, S.; Kincaid, J. R.; Czarnecki, K.; Hemley, R. J. *PANS* **2002**, *99*, 12526.
- (51) Drobizhev, M.; Karotki, A.; Kruk, M.; Mamardashvili, N. Zh.; Rebane, A. *Chem. Phys. Lett.* **2002**, *361*, 504.
- (52) Nesbitt, D. J.; Field, R. W. *J. Phys. Chem.* **1996**, *100*, 12735.